

Excited-State Intramolecular Proton Transfer and Rotamerism of 2-(2'-hydroxyvinyl)benzimidazole and 2-(2'-hydroxyphenyl)imidazole

M. Forés,[†] M. Duran,[†] M. Solà,[†] and L. Adamowicz^{*,‡}

Institut de Química Computacional and Departament de Química, Universitat de Girona, 17071 Girona, Catalonia, Spain, and Department of Chemistry, University of Arizona, Tucson, Arizona 85721

Received: November 18, 1998; In Final Form: February 16, 1999

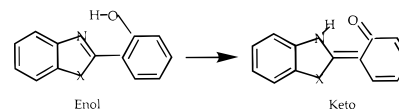
The intramolecular proton transfer of 2-(2'-hydroxyvinyl)benzimidazole (HVBI) and 2-(2'-hydroxyphenyl)imidazole (HPI) in the ground state and in the $^1\pi\pi^*$, $^1n\pi^*$, and $^3\pi\pi^*$ excited states has been studied at the HF/CIS/D95** level of theory. Their rotamerism reaction in the ground and $^1\pi\pi^*$ excited states has been also analyzed. These systems are two different fragments of 2-(2'-hydroxyphenyl)benzimidazole (HPBI), containing an intramolecular hydrogen bond through a common NCCCCO backbone. The comparison of the calculations on HVBI and HPI with the experimental results available for HPBI and the theoretical calculations done for HPBI, salicyaldimine, and 1-amino-3-propenal allow us to determine the influence that each functional group of HPBI has on its intramolecular proton transfer in different electronic states. It is found that the aromaticity of the phenol ring of HPBI exerts a great influence on the proton transfer in the ground state and the lowest-lying $^1\pi\pi^*$, and $^3\pi\pi^*$ excited states. The aromatic character of the phenol ring explains the higher stability of the enol form with respect to the keto form in the ground state, while a change in its aromaticity is responsible for the shift in the relative stability of the two tautomeric forms in the $^1\pi\pi^*$, and $^3\pi\pi^*$ excited states. The presence of the imidazole moiety stabilizes the keto form in the $^1n\pi^*$ excited state, exerting a significant influence on the proton transfer in this state.

Introduction

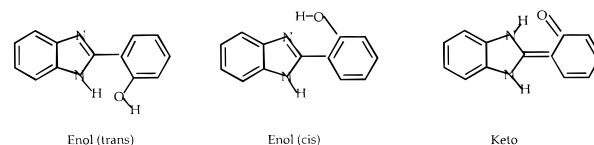
The importance of the intramolecular proton transfer in the photophysical and photochemical properties of systems such as 2-(2'-hydroxyphenyl)benzoxazole (X = O, HPBO),^{1–6} 2-(2'-hydroxyphenyl)benzothiazole (X = S, HPBT),^{6–10} 2-(2'-hydroxyphenyl)benzimidazole (X = NH, HPBI)^{11–14} (see Scheme 1), and related compounds has been well established.^{15–30} An important common feature shared by these compounds is the phenol group which is hydrogen bonded to a nitrogen atom of the same molecule. Photoexcitations in these systems usually lead to radical changes in the electron density of their acidic and basic centers^{13,31–36} that facilitate the transference of the H atom from the OH group to the adjacent N atom and the formation of phototautomers. This is usually a very fast process since it occurs within a few picoseconds even in molecules deposited in rigid matrixes at 4 K.^{16,18,19} The above-mentioned molecules can be used as effective photoprotecting agents,^{1,11,37,38} triplet quenchers,³⁹ and laser dyes.^{26,40–46}

A large Stokes shift from the keto tautomer followed by a normal emission from the enol form is usually registered in the emission spectrum of the species shown in Scheme 1.^{11,14,16,18,19,24–26} Particularly, a strong normal emission along with a tautomer emission was reported for HPBI in polar solvents.^{11–14,24,47} This can be explained by the coexistence of two intramolecularly hydrogen-bonded rotamers in the ground state, the enol (cis) and the enol (trans) forms (see Scheme 2). The rotamer interconversion involves breaking of the intramolecular hydrogen bond in the enol (cis) form and a rotation by 180° around the C–C bond that links the benzimidazole and

SCHEME 1



SCHEME 2



phenol moieties. It was showed that the phototautomer is only obtained upon an electronic excitation of the enol (cis) form and that the enol (trans) form, which is responsible for the normal emission, does not undergo an excited-state intramolecular proton transfer (ESIPT) reaction.^{12,13}

From a theoretical point of view, it is well established that an accurate evaluation of the energy parameters governing the proton transfer requires the use of large basis sets and the inclusion of electron correlation effects. For this reason, the theoretical study of these experimentally very interesting molecules is usually impractical and it is often performed in molecular models of reduced size. Thus, it is really important to find the right simple molecular model able of reproducing, at least qualitatively, the ESIPT process that takes place in the modeled system. For HPBO, HPBT, and HPBI, 1-amino-3-propenal (1A3P) is the simplest model to study their intramolecular proton transfer in the ground and excited states.^{48,49} However, the analysis of the intramolecular proton transfer in a larger system such as salicyaldimine (SA) (see Scheme 3), which contains an aromatic phenol ring, revealed important differences in the relative stability of the two tautomers and in the proton-transfer

* To whom correspondence should be addressed.

[†] Universitat de Girona.

[‡] University of Arizona.

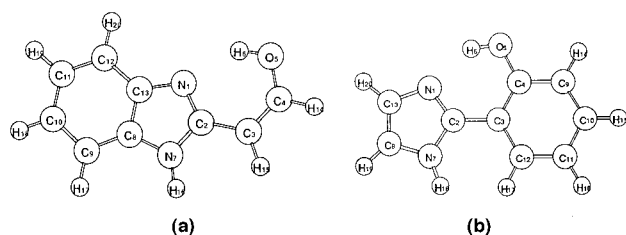
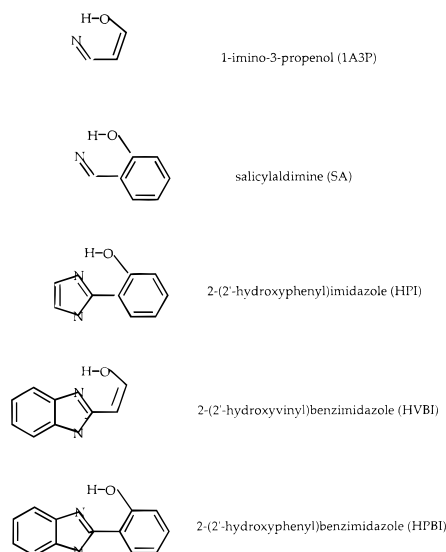


Figure 1. The ground state optimized geometries of the enol (cis) form of (a) HVBI and (b) HPI species.

SCHEME 3



barriers between 1-amino-3-propenal and salicylaldehyde. This put forward that the results obtained from small models do not always apply to larger systems⁴⁹ and that a wrong election of the molecular model can lead to erroneous conclusions.

In the present work we have analyzed how different molecular fragments of HBPI affect the intramolecular proton transfer in the ground state and the lowest-lying ${}^1\pi\pi^*$, ${}^1n\pi^*$, and ${}^3\pi\pi^*$ excited states. The aim is to determine which is the smallest molecular model that exhibits qualitatively the same photochemical behavior as HPBI and to study the effect that the different molecular fragments have on the ESIPT processes of HPBI. In particular, the effect of the phenol, imidazole, and benzimidazole rings of HPBI on its ESIPT processes has been analyzed. Two model systems of HPBI, 2-(2'-hydroxyvinyl)benzimidazole (HVBI), and 2-(2'-hydroxyphenyl)imidazole (HPI) (Scheme 3 and Figure 1) have been chosen for the present analysis. The former differs from HPBI by the lack of the phenol ring while the phenyl ring of HPBI has been removed in the latter. Comparison of the results for these two systems, in combination with previous theoretical results of 1-amino-3-propenal and salicylaldehyde⁴⁹ and theoretical^{50,51} and experimental^{11-14,24,47} results of HPBI, has allowed the elucidation of the role that each molecular fragment of HPBI plays in the intramolecular proton transfer in the ground and excited electronic states. Moreover, since the enol (trans) is responsible for the strong normal emission in HPBI,^{12,13} the rotamerism between the enol (cis) and the enol (trans) of HVBI and HPI in the ground state and the first singlet excited state has been also analyzed.

Computational Details

All molecular geometries in this work have been fully optimized at the restricted Hartree–Fock (RHF) level in the

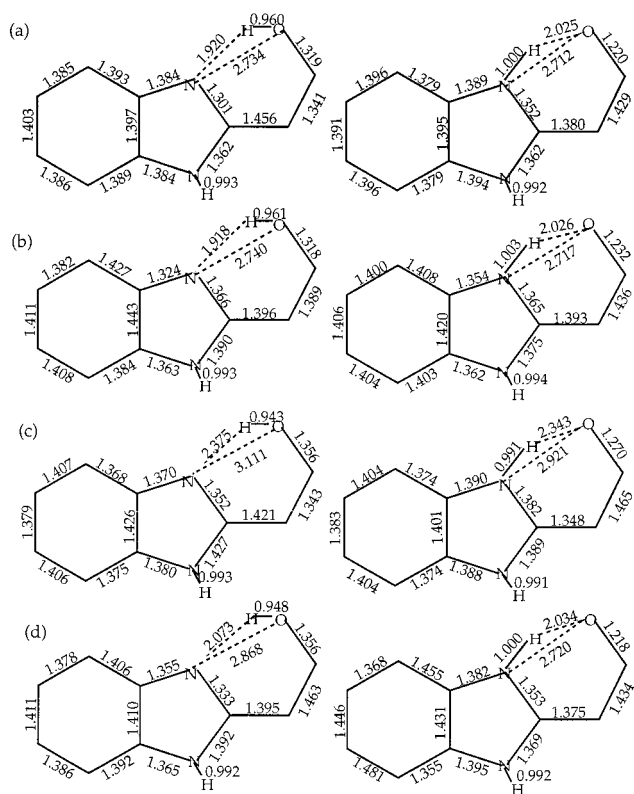


Figure 2. Geometrical parameters of the enol (on the left) and keto (on the right) forms of HVBI in the (a) ground state, (b) ${}^1\pi\pi^*$, (c) ${}^1n\pi^*$, and (d) ${}^3\pi\pi^*$ excited states.

ground state, while the configuration interaction all single-excitations method (CIS)⁵² with the spin-restricted Hartree–Fock reference ground state has been employed to optimize the geometries in the excited states. Core electrons have not been correlated in the CIS calculations. All located transition states exhibit the expected normal imaginary frequency with a transition vector that corresponds to the motion of atoms during the proton transfer process. Despite the well-known fact that CIS usually overestimates the energy barrier for the proton transfer and fails to describe a more significant bond breaking,⁵³⁻⁵⁸ the CIS method has been employed because it was demonstrated that it provides a qualitatively correct characterization of the ESIPT processes.^{49,50,57} The calculations have been carried out with the Gaussian 94 program⁵⁹ using the double- ζ Gaussian basis set of Dunning and Hay with polarization functions (D95**).⁶⁰

Results and Discussion

2-(2'-Hydroxyvinyl)benzimidazole (HVBI). The geometrical parameters most relevant to the present discussion of the enol (cis) and the keto forms of HVBI optimized in the ground state and in the lowest-lying ${}^1\pi\pi^*$, ${}^1n\pi^*$, and ${}^3\pi\pi^*$ excited states are plotted in Figure 2. In the ground state, the single and double C–C bond distances of the phenyl ring in the enol (cis) and keto forms are quite close to each other because of the similar aromaticity of their phenyl rings. In fact, taking the difference between the largest and the smallest C–C bond distance of the phenyl ring (η) as a measure of the degree of aromaticity,^{61,62} we find that η is 0.017 Å for both tautomers. Also, only a few differences were found among the C–C bond distances of the phenyl ring in the two tautomers of HPBI optimized at the RHF level with the 3-21G*⁵⁰ and D95**⁵¹ basis sets. The bond distances of the imidazole moiety in the enol (cis) form are

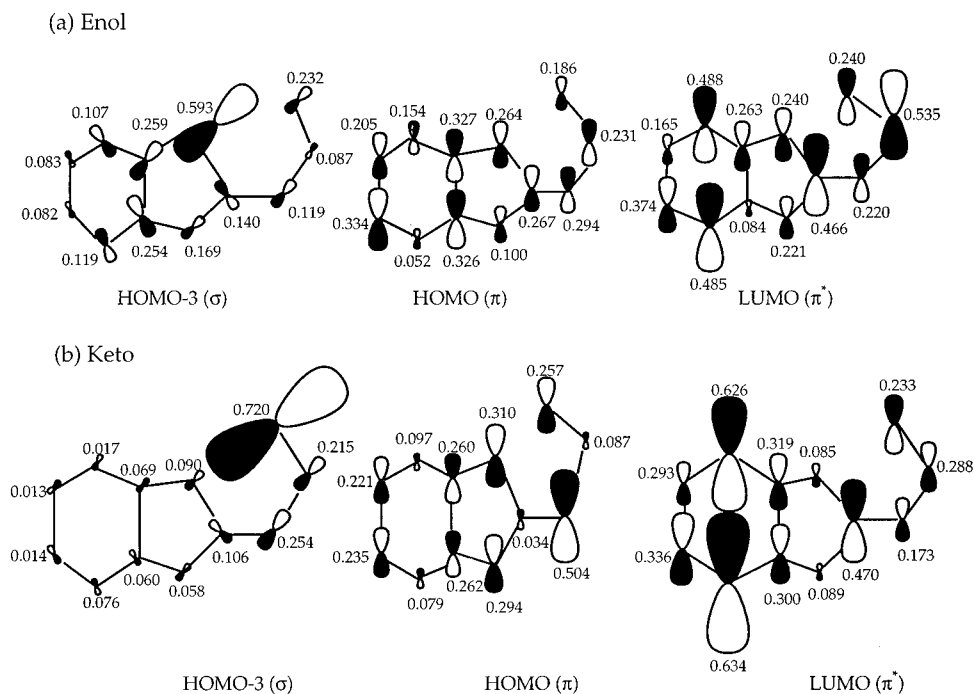


Figure 3. Schematic diagram of the orbital structure of the HOMO-3 (σ), HOMO (π), and LUMO (π^*) for the (a) enol and (b) keto tautomers of HVBI. The numbers correspond to the value of the molecular orbital coefficient obtained from the square root of the sum of the squared coefficients of intervening atomic orbitals.

also similar to the corresponding bond distances in the keto form, except for the N_1-C_2 bond length (see Figure 1 for atom numbering). The N_1-C_2 bond length in the enol form is smaller than in the keto form because it is formally a double bond in the former and a single bond in the latter.

The first singlet excited state corresponds to an excitation of an electron from the HOMO π orbital to the antibonding LUMO π orbital. The second singlet excited state corresponds to a one-electron excitation from the HOMO-3 σ orbital to the LUMO π orbital. Qualitative molecular orbital representations of the HOMO-3, HOMO, and LUMO orbitals of the enol (cis) and keto forms are presented in Figure 3. An electronic excitation results in some electron density redistribution that affects the molecular geometry. In general, a correlation is found between the change in the bonding character of the orbitals involved in the electronic transition for each pair of bonded atoms and the change in the corresponding bond distance. Remarkably, the nodal structure of the orbitals involved in the $^1\pi\pi^*$ excitation in the benzimidazole fragment is similar in the two tautomers, and this is reflected in the similar geometry changes of the benzimidazole group of the enol and keto forms in the $^1\pi\pi^*$ photoexcitation.

The N_1-H_6 , H_6-O_5 , and the N_1-O_5 bond distances of the enol and keto forms in the ground state are similar to the corresponding bond distances of the enol and keto forms in the $^1\pi\pi^*$ state. This indicates that the strength of the hydrogen bond is almost unaffected by the $^1\pi\pi^*$ excitation. Similar results are obtained for the $^3\pi\pi^*$ excitation, although larger N_1-H_6 and N_1-O_5 bond distances in the enol form of this state reveal that the hydrogen bond strength has been reduced following photoexcitation to the $^3\pi\pi^*$ excited state.

As in 1-amino-3-propenal,⁴⁹ after the $^1n\pi^*$ photoexcitation there is an important reduction of the electron density in the basic center of the enol and keto forms of HVBI that translates into a reduction on the hydrogen bond strength in both tautomers. For instance, the Mulliken populations of N_1 , H_6 , and O_5 atoms in the ground state of the enol form are -0.430 ,

TABLE 1: Energy Difference (ΔE_{E-K}) between the Two Tautomeric Forms of HVBI and Direct (ΔE_{E-K}^{TS}) and Reverse (ΔE_{K-E}^{TS}) Energy Barriers for the Proton Transfer in the S_0 , $^1\pi\pi^*$, $^1n\pi^*$, and $^3\pi\pi^*$ States

	ΔE_{E-K}^a	$\Delta E_{E-K}^{TS,a}$	$\Delta E_{K-E}^{TS,a}$
S_0	-1.8	12.5	10.6
$^1\pi\pi^*$	-2.6	13.1	10.6
$^1n\pi^*$	+37.6	10.6	48.3
$^3\pi\pi^*$	-11.7	24.0	12.3

^a In kcal/mol.

0.409, and -0.463 electrons and in the $^1n\pi^*$ state they change to 0.123, 0.391, and -0.486 electrons, respectively.

The energy difference between the two tautomeric forms (negative values indicate that the enol form is more stable than the keto form) and the forward and reverse energy barriers for the proton transfer that transforms the enol (cis) to the keto form are reported in Table 1. The enol and the keto forms of HVBI are almost isoenergetic in the ground state. The similar stability of these two forms in the ground state can be understood on the basis of similarities in their electronic structures, as described before. The situation is quite different in HPBI, where in the ground state the enol form is more stable than the keto form by 7.3 kcal/mol at the HF/3-21G⁵⁰ level and by 13.1 kcal/mol with the HF/D95⁵¹ method. The larger stability of the enol form in the ground state of HPBI is due to the existence of the aromatic phenol ring in the enol form that is not present in its keto tautomer.⁴⁹

Also, the shift in the energy difference between the two tautomers of HPBI upon $^1\pi\pi^*$ excitation^{50,51} is not apparent in HVBI. The enol of HVBI in the $^1\pi\pi^*$ state is stabilized with respect to the keto form by nearly the same amount of energy as in the ground state. In the $^3\pi\pi^*$ state, the enol form of HVBI is noticeably more stabilized than in the keto form. In this electronic excitation, the η parameter for the phenyl ring of HVBI increases by 0.016 and 0.109 Å for the enol and keto forms, respectively, indicating a larger loss of aromaticity in the phenyl ring of the keto form than in that of the enol form

TABLE 2: Geometry Parameters (in Å) Involved in the Hydrogen Bond of the Enol (trans) Form of HVBI, Energy Difference between the Enol (cis) and the Enol (trans) ($\Delta E_{\text{Ec-Et}}$) Forms, and Direct ($\Delta E_{\text{Ec-Et}}^{\text{TS}}$) and Reverse ($\Delta E_{\text{Et-Ec}}^{\text{TS}}$) Energy Barriers for the Rotational Process in the Ground and the ${}^1\pi\pi^*$ States

	$\text{N}_7\text{-H}_{16}$	$\text{H}_{16}\text{-O}_5$	$\text{N}_7\text{-O}_5$	$\text{O}_5\text{-H}_6$	$\Delta E_{\text{Ec-Et}}^a$	$\Delta E_{\text{Ec-Et}}^{\text{TS}a}$	$\Delta E_{\text{Et-Ec}}^{\text{TS}a}$
S_0	0.993	2.225	2.834	0.943	-7.3	11.9	4.5
${}^1\pi\pi^*$	0.994	2.215	2.821	0.944	-7.0	23.8	16.9

^a In kcal/mol.

after ${}^3\pi\pi^*$ excitation. On the contrary, the keto form is more stabilized than the enol tautomer in the ${}^1n\pi^*$ state. This result was also found in 1-amino-3-propenal⁴⁹ and can be understood by analyzing the orbitals involved in the excitation. The LCAO MO coefficients of the σ orbital of the enol tautomer shown in Figure 3 are quite different from those of the keto form. According to these coefficients, the electron density is less concentrated at the N atom in the enol form than at the O atom in the keto form. Therefore, when an electron is promoted from the σ orbital to the π^* orbital, the destabilization effect is smaller in the keto form because of the larger reduction in electron–electron repulsions upon the electronic excitation. In addition, the loss of aromaticity in the phenyl ring of HVBI is more important in the enol than in the keto tautomer (the η parameter is 0.058 Å for the enol form and 0.030 Å for the keto form). Remarkably, the ${}^1n\pi^*$ excitation of the enol form corresponds to the third excited state of this system, while for the keto form it corresponds to the first excited state. This crossing between the ${}^1\pi\pi^*$ and ${}^1n\pi^*$ excited states, also observed in 1-amino-3-propenal,^{48,49} may open a channel for inhibition of the ESIPT process after the keto promotion to the ${}^1\pi\pi^*$ excited state. That is, the keto form promoted to the ${}^1\pi\pi^*$ excited state can follow the adiabatic potential energy curve falling down to the ${}^1n\pi^*$ excited state and returning to the ground state before giving rise to the enol form in the ${}^1\pi\pi^*$ excited state.

The similarities between the ground and ${}^1\pi\pi^*$ excited states are also reflected in the similar energy barriers found for the proton transfer in the enol and the keto forms in these states. This is completely different in salicylaldimine⁴⁹ and HPBI,⁵⁰ where the proton transfer is favored in the ${}^1\pi\pi^*$ state as compared to the ground state. Interestingly, the ${}^3\pi\pi^*$ state also differs from the ${}^1\pi\pi^*$ state in the proton-transfer barrier. The barrier for the proton transfer of the enol form in the ${}^3\pi\pi^*$ state is about 11 kcal/mol higher than in the ${}^1\pi\pi^*$ state. This result is consistent with the reduction of the intramolecular hydrogen bond strength found in the ${}^3\pi\pi^*$ excitation. Despite the fact that the hydrogen bond strength is also diminished in both tautomers after the ${}^1n\pi^*$ excitation, the smallest barrier to the proton transfer from the enol to the keto form is found for this excited state. This result is attributed to the high exothermicity of the enol to keto conversion in this state.

Table 2 lists the geometrical parameters describing the structure of the intramolecular hydrogen bond in the enol (trans) form and the energy difference between the enol (cis) and enol (trans) forms (negative values indicate that the enol (cis) is more stable than the enol (trans)). Also, the direct and reverse energy barriers for the rotation process in the ground and the ${}^1\pi\pi^*$ states are given in the table. Since the H_6 atom in the enol (trans) form is far from the N_1 atom, the $\text{O}_5\text{-H}_6$ bond distance becomes shorter in the enol (trans) than in the enol (cis). On the other hand, despite that the H_{16} atom forms a hydrogen bond with the O_5 atom in the enol (trans), the $\text{N}_7\text{-H}_{16}$ bond distance hardly changes in going from the enol (cis) to the enol (trans). Moreover, the $\text{N}_7\text{-O}_5$ bond length is larger in the enol (trans) form than the $\text{N}_1\text{-O}_5$ bond length in the enol (cis) form. These results indicate that the intramolecular hydrogen bond present in the enol (trans) form is weaker than in the enol (cis) structure.

The larger stability (by 7.3 kcal/mol in HPVI and by 4.2 kcal/mol in HPBI⁵¹) of the enol (cis) form with respect to the enol (trans) conformer can be attributed to the stronger $\text{O}_5\text{H}_6\cdots\text{N}_1$ hydrogen bond as compared to the $\text{O}_5\cdots\text{H}_{16}\text{N}_1$ hydrogen bond as a result of the better proton donating ability of O and accepting capacity of N.

In nonpolar solvents, HPBI is present as a unique enol (cis) conformer.^{12–14} In water the enol (trans) is stabilized with respect to the enol (cis) and HPBI exists as a mixture of these two interconvertible rotamers in the ground state.^{11–14,24,47} The results obtained for HVBI indicate that the rotamer interconversion for this system in the ground state will be more difficult irrespective of the solvent used. As in HPBI,¹² the HVBI rotamer interconversion in the ${}^1\pi\pi^*$ excited state is prevented by a higher energy barrier than in the ground state. Since the lifetime of these systems in the excited state is rather short, after the electronic excitation of the enol (cis) form, it will either relax back to the ground state or undergo an ESIPT before the cis–trans rotation takes place.

2-(2'-Hydroxyphenyl)imidazole (HPI). According to the Lewis structures, the enol and the keto tautomers of HPI have different distribution of the single and double bonds. Unlike the keto form, the enol form has an aromatic six-membered ring and a larger π delocalization that expands over the imidazole ring. These differences are reflected in the bond lengths of the two tautomers in the ground state, as shown in Figure 4. All of the C–C bond distances in the phenyl ring of the enol (cis) form are within 0.02 Å of each other, while the bond lengths in the ring of the keto form clearly show a single/double bond alteration of the bonds (they range between 1.45 and 1.35 Å). Similar behavior was found in the two tautomers of salicylaldimine⁴⁹ and HPBI.^{50,51} Furthermore, the imidazole rings in the enol and keto tautomers exhibit some noticeable differences. Despite being formally a double bond in both tautomers, the $\text{C}_8\text{-C}_{13}$ bond in the enol form is 0.014 Å larger than in the keto form. On the other hand, the $\text{N}_7\text{-C}_8$ bond, formally single in both tautomers, is 0.014 Å smaller in the enol form than in the keto form. We attribute these geometrical differences to a larger electron delocalization in the enol than in the keto form.

As in salicylaldimine,⁴⁹ HPBI,^{50,51} and HVBI, when one electron is transferred from the HOMO orbital of HPI to the LUMO orbital, the first singlet ${}^1\pi\pi^*$ excited state is formed. When a one-electron transition takes place between the highest occupied σ orbital and the LUMO orbital, the second singlet excited state is obtained (see Figure 5 for orbital representation). The ${}^1\pi\pi^*$ excitation of the enol form leads to some lengthening of the C–C bond distances around the six-membered ring (the exceptions are the $\text{C}_4\text{-C}_9$ and $\text{C}_{11}\text{-C}_{12}$ bond distances) and some loss of aromaticity (the η value for the phenol ring increases by 0.074 Å in the ${}^1\pi\pi^*$ photoexcitation). By contrast, the bond lengths of the ring in the keto form increase and reduce alternately becoming more uniform (although in this case the η value remains almost constant). This result agrees with that found for salicylaldimine.⁴⁹ On the other hand, the bond distances of the imidazole moiety in both tautomers behave similarly upon the ${}^1\pi\pi^*$ excitation, although the change is more

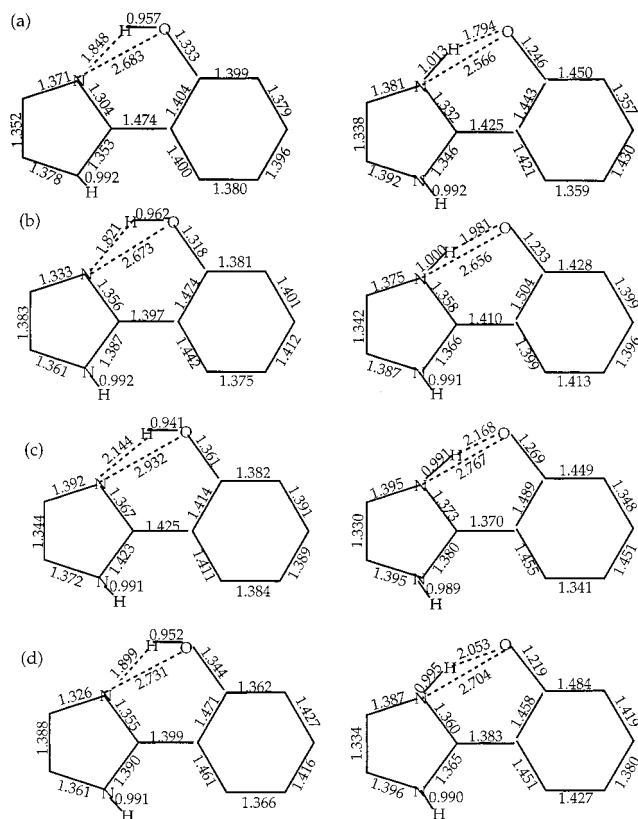


Figure 4. Geometrical parameters of the enol (on the left) and the keto (on the right) forms of HPI in the (a) ground state, (b) ${}^1\pi\pi^*$, (c) ${}^1n\pi^*$, and (d) ${}^3\pi\pi^*$ excited states.

significant in the enol form. Also, the structural changes in the two tautomers of 2-(2'-hydroxyphenyl)oxazole (HPO) in the ${}^1\pi\pi^*$ excited state follow a similar pattern.⁶³

Among the geometrical parameters that change the most in the process of proton transfer, the O_5-H_6 and N_1-O_5 bond distances of the keto form are larger in all excited states than in the ground state. This indicates that the hydrogen bond in this tautomer is stronger in the ground state than in the excited states. A similar effect occurs in the ${}^1n\pi^*$ and ${}^3\pi\pi^*$ excited states for the enol form. However, the distance between the N_1 and the H_6 atoms for the enol form in the ${}^1\pi\pi^*$ excited state is shorter than in the ground state, indicating that the strength of the hydrogen bond increases upon the ${}^1\pi\pi^*$ excitation. The same result was found for 1-amino-3-propenal,⁴⁹ salicylaldehyde,⁴⁹ and HPBI.⁵⁰

The energy parameters concerning the keto-enol tautomerism in HPI are given in Table 3. The enol tautomer is more stabilized than the keto form in the ground state, and the difference in energy between the two tautomers is about 13 and 9 kcal/mol smaller than in HVBI and salicylaldehyde,⁴⁹ respectively, but only 2 kcal/mol smaller than in HPBI.⁵¹ The aromaticity of the enol form and the lack of it in the keto form are responsible for the higher stability of the former tautomer.^{49,63} The imidazole moiety appears also to stabilize the enol form in the ground state. The enol form of HPI in the ${}^1\pi\pi^*$ excited state is less stable than the keto form. As in salicylaldehyde⁴⁹ and HPBI,⁶³ there is a reverse of the relative stability of the two tautomers upon the ${}^1\pi\pi^*$ excitation. This change in stability comes from the enol form losing aromaticity and the keto form gaining it.⁴⁹ The keto tautomer of HPI in the ${}^1\pi\pi^*$ excited state is stabilized with respect to the enol form by an amount similar to that in HPBI^{50,51} but by a smaller quantity than in salicylaldehyde.⁴⁹ The similarities between the relative stability of the two

tautomers of HPI and HPBI in both the ground and ${}^1\pi\pi^*$ states indicate that the phenyl ring exerts little influence on their stability.

Although the energy barrier for the proton transfer is reduced by 8.3 kcal/mol after ${}^1\pi\pi^*$ excitation in HPI, it is still too high to facilitate an ultrafast ESIPT in this state such as it was experimentally observed in HPBI¹¹⁻¹⁴ or theoretically predicted for HPBI⁵⁰ and salicylaldehyde.⁴⁹ Including electronic correlation in the calculation should reduce the proton-transfer energy barrier in the ${}^1\pi\pi^*$ state and improve the agreement with the experimental results, as was shown by salicylaldehyde⁴⁹ and HPO.⁶³ Furthermore, it was shown experimentally that HPI derivatives exhibit features similar to HPBI,⁶⁴ and this corroborates our conclusions concerning HPI. The HPI results and those obtained for HPO⁶³ are consistent with the relation between the electronegativity of the X atom and the energy barrier established for the series of compounds, HPBI, HPBO, and HPBT.⁵⁰ This relation states that the energy barrier for the proton transfer from the enol to the keto tautomer increases with the electronegativity of X. In agreement with that, the HF/CIS/6-31G* energy barriers for the proton transfer from the enol to the keto tautomer in HPO (X = O) are 22.1 and 10.7 kcal/mol for the ground and ${}^1\pi\pi^*$ states,⁶³ respectively, while these barriers for HPI (X = NH), computed with the HF/CIS/D95** method, are 17.6 and 9.3 kcal/mol, respectively.

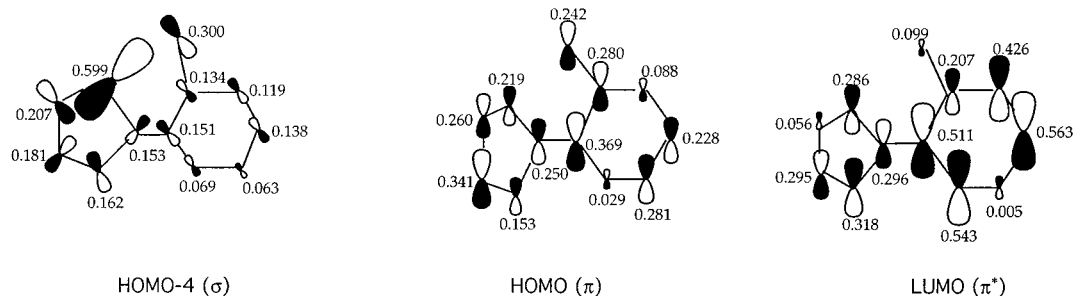
Finally, let us analyze the internal rotation in HPI (Table 4). Geometrically and energetically the rotation process of HPI follows a pattern similar to that of HVBI. The hydrogen bond in the enol (trans) form appears weaker than in the enol (cis) form. The enol (cis) is more stable than the enol (trans) in both the ground and the ${}^1\pi\pi^*$ states, and the energy barrier is higher in the ${}^1\pi\pi^*$ state than in the ground state. However, the interconversion between the two conformers of HPI in the ground state is more feasible than in HVBI. It should be mentioned that, in agreement with our results, the predominance of the enol (cis) rotamer of HPI in the ground state was recently determined experimentally.⁶⁵

A Comparison between ESIPT Process in a Series of Different Models of 2-(2'-Hydroxyphenyl)benzimidazole (HPBI). Table 5 collects the energy differences between the keto and enol forms, the difference between the relative stability of the two tautomers in the ground state and each excited state, and the energy barriers for the enol to keto conversion in different electronic states of a series of HPBI fragments.

As far as the ground state is concerned, the phenol ring is a critical fragment for the relative stability of the two tautomers. All systems containing the phenol ring have a ground-state enol form more stable than the keto tautomer due to the presence of the aromatic phenol ring in the former. In HVBI, the two tautomers have similar energies. Compared to 1A3P, the benzimidazole group in HVBI acts to stabilize the enol form by ca. 10 kcal/mol. Again the larger π electron delocalization in the enol form than in the keto form explains the greater stability of the HVBI enol tautomer. This effect also accounts for the greater stability of the enol with respect to the keto form in HPI when compared to SA. The energy barriers increase with the endothermicity of the enol to keto conversion process. The only exception is HPBI, but it must be said that the barrier of 9.5 kcal/mol reported in Table 5 was computed with the HF/3-21G* method.⁵⁰ At the HF/D95** level, the energy barrier for the conversion of the enol to the keto form must be necessarily larger than 13.1 kcal/mol.

Among the excited states studied, the ${}^1\pi\pi^*$ excited state is the only one that has significant oscillator strength and therefore

(a) Enol



(b) Keto

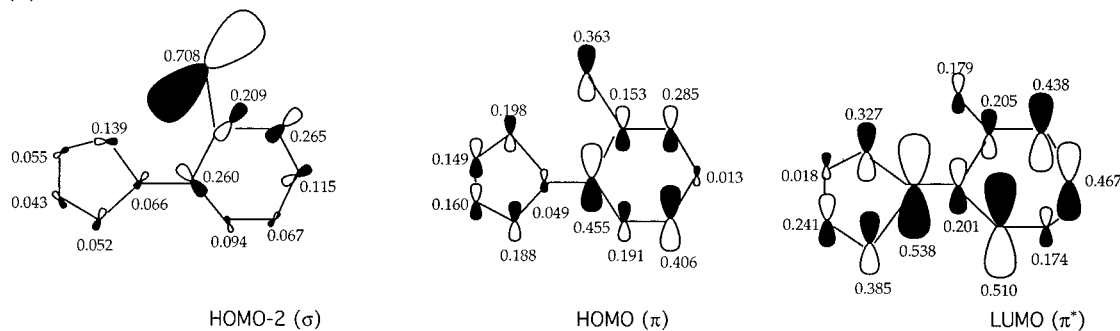


Figure 5. Schematic diagram of the orbital structure of the HOMO-4 (σ), HOMO (π), and LUMO (π^*) for the (a) enol and the HOMO-2 (σ), HOMO (π), and LUMO (π^*) and for (b) the keto tautomers of HPI. The numbers correspond to the value of the molecular orbital coefficient obtained from the square root of the sum of the squared coefficients of intervening atomic orbitals.

TABLE 3: Energy Difference (ΔE_{E-K}) between the Two Tautomeric Forms of HPI and Direct (ΔE_{E-K}^{TS}) and Reverse (ΔE_{K-E}^{TS}) Energy Barriers for the Proton Transfer in the S_0 , ${}^1\pi\pi^*$, ${}^1n\pi^*$, and ${}^3\pi\pi^*$ States

	ΔE_{E-K}^a	ΔE_{E-K}^{TSa}	ΔE_{K-E}^{TSa}
S_0	-15.1	17.6	2.5
${}^1\pi\pi^*$	3.0	9.3	12.3
${}^1n\pi^*$	20.1	15.4	35.5
${}^3\pi\pi^*$	-3.3	17.7	14.4

^a In kcal/mol.

is the state that has the largest relevance from an experimental point of view. Remarkably, all systems having a phenol ring experience a reverse of the stability of the two tautomers upon the ${}^1\pi\pi^*$ excitation. The energy change in the stability of the two tautomers is 16.3, 18.1, and 23.8 kcal/mol in the HPBI, HPI, and SA systems, respectively. This property together with the high fluorescence yields and the low barrier for the proton transfer in the ${}^1\pi\pi^*$ state are the basis for the efficient laser action found in HPBI.^{24,45,46} Systems that do not show this behavior cannot be considered good models of HPBI. As commented before, the change in the relative stability of the enol and keto forms following ${}^1\pi\pi^*$ excitation is attributed to a loss of aromaticity in the phenol ring of the enol form and a gain of aromatic character in that of the keto tautomer. The relative stability of the enol with respect to the keto form in the ${}^1\pi\pi^*$ transition is not much affected by the presence of the imidazole and benzimidazole groups. For instance, whereas in 1A3P the keto tautomer is stabilized by only 0.3 kcal/mol in this transition, in HVBI it is the enol form that is stabilized by only 0.8 kcal/mol.

In the ${}^1n\pi^*$ transition, the keto form of all systems is stabilized with respect to the enol form. As commented before, this can be attributed to the larger reduction in electron–electron repulsions experienced by the keto form in this transition. In

this case, the phenol ring seems to have an opposite effect although it is not very significant. For instance, the keto is stabilized by 7.7 kcal/mol in 1A3P and by 6.6 kcal/mol in SA. Likewise, the keto is stabilized by 35.2 kcal/mol in HPI and by 39.4 kcal/mol in HVBI. In this transition, the fragment that has the largest influence is the imidazole or benzimidazole groups. Their presence stabilizes the keto form by 35–40 kcal/mol. This can be related to the larger localization of the nonbonding oxygen lone pair for systems that contain the imidazole or benzimidazole group. According to this finding, it is expected that the relative energy between the two tautomers of HPBI will be closer to that of HVBI than to that of HPI.

Finally, comparing the difference between the relative stability of the two tautomers in the ground state and the ${}^3\pi\pi^*$ state for 1A3P and HVBI (−8.6 and −9.9 kcal/mol, respectively) one can say that there is a slight stabilization of the enol form owing to the presence of the benzimidazole group in the molecule. By contrast, the phenol ring helps to stabilize strongly the keto form, as happens in the ${}^1\pi\pi^*$ state.

Conclusions

A detailed analysis of the proton transfer in the HVBI and the HPI systems in the ground and the ${}^1\pi\pi^*$, ${}^1n\pi^*$, and ${}^3\pi\pi^*$ excited states has been performed. The results have been compared with the calculations of 1A3P and SA and with the available theoretical and experimental results for HPBI. Rotamerism of HVBI and HPI in the ground and the ${}^1\pi\pi^*$ states has been also investigated.

The two tautomers of HVBI are structurally very similar and almost equally stable in the ground state. By contrast, the energy difference between the enol and keto forms of HPI in the ground state is predicted to be quite large. Unlike the keto form of HPI, the enol form exhibits aromaticity in the six-membered ring. This effect stabilizes the enol tautomer more than the keto tautomer.

TABLE 4: Geometry Parameters (in Å) Involved in the Hydrogen Bond of the Enol (trans) Form of HPI, the Energy Difference between the Enol (cis) and the Enol (trans) ($\Delta E_{\text{Ec-Et}}$) Forms, and Direct ($\Delta E_{\text{Ec-Et}}^{\text{TS}}$) and Reverse ($\Delta E_{\text{Et-Ec}}^{\text{TS}}$) Energy Barriers for the Rotational Process in the Ground and the $^1\pi\pi^*$ States

	N ₇ -H ₁₆	H ₁₆ -O ₅	N ₇ -O ₅	O ₅ -H ₆	$\Delta E_{\text{Ec-Et}}^a$	$\Delta E_{\text{Ec-Et}}^{\text{TS}^a}$	$\Delta E_{\text{Et-Ec}}^{\text{TS}^a}$
S ₀	0.993	2.096	2.721	0.944	-3.9	8.3	4.4
$^1\pi\pi^*$	0.993	2.114	2.721	0.945	-4.1	25.9	21.8

^a In kcal/mol.**TABLE 5: HF/CIS/D95** Energy Difference ($\Delta E_{\text{E-K}}$) between the Two Tautomeric Forms of Different Models of HPBI, the Difference of the Relative Stability of the Two Tautomers in Each Electronic Excitation ($\Delta\Delta E_{\text{E-K}}$), and Direct ($\Delta E_{\text{E-K}}^{\text{TS}}$) Energy Barrier for the Proton Transfer in the S₀, $^1\pi\pi^*$, $^1n\pi^*$, and $^3\pi\pi^*$ Excited States**

	$\Delta E_{\text{E-K}}^a$	$\Delta\Delta E_{\text{E-K}}^a$	$\Delta E_{\text{E-K}}^{\text{TS}^a}$
S ₀			
1A3P ^b	8.7	0.0	8.7
SA ^b	-6.8	0.0	14.4
HPI	-15.1	0.0	17.6
HVBI	-1.8	0.0	12.5
HPBI ^c	-13.1	0.0	9.5 ^d
$^1\pi\pi^*$			
1A3P ^b	9.0	0.3	3.5
SA ^b	17.0	23.8	1.5
HPI	3.0	18.1	9.3
HVBI	-2.6	-0.8	13.1
HPBI ^c	3.2	16.3	2.3 ^d
$^1n\pi^*$			
1A3P ^b	16.4	7.7	26.7
SA ^b	-0.2	6.6	25.2
HPI	20.1	35.2	15.4
HVBI	37.6	39.4	10.6
HPBI			
$^3\pi\pi^*$			
1A3P	0.1	-8.6	26.1
SA ^c	14.6	21.4	14.1
HPI	-3.3	11.8	17.7
HVBI	-11.7	-9.9	24.0
HPBI			

^a In kcal/mol. ^b Results from ref 49. ^c Results from ref 51. ^d Computed at the HF/CIS/3-21G* level from ref 50. ^e Results from ref 62.

The $^1\pi\pi^*$ excitation exerts a similar effect on the enol and keto forms of HVBI and, as a consequence, the proton transfer in the $^1\pi\pi^*$ state is similar to that found in the ground state. On the other hand, HPI behaves similarly to HBPI and salicylaldimine in the $^1\pi\pi^*$ excited state, i.e., the energy barrier for the proton transfer decreases upon the excitation. The aromaticity gain by the ring in the keto form increases the stability of this tautomer with respect to the enol form.

HVBI and HPI show similar features for the proton transfer in the $^1n\pi^*$ state. The keto form is quite more stable than the enol form. This is explained by differences in the σ orbitals of the enol and keto forms. The σ orbital in the keto form describes basically the nonbonding oxygen lone pair, while in the enol form this orbital is more spread over the whole molecule. Hence, the keto form is less destabilized than the enol form by the $^1n\pi^*$ excitation.

Some differences are found in the proton transfer of HVBI and HPI in the $^3\pi\pi^*$ state. Whereas the relative stability of the enol and keto forms and the energy barrier of HVBI increase upon $^3\pi\pi^*$ excitation, the two tautomers of HPI become closer in energy and the energy barrier hardly changes.

Summarizing, the phenol ring is essential to describe the intramolecular proton transfer of HPBI in the ground, $^1\pi\pi^*$, and $^3\pi\pi^*$ excited states while the imidazole is the fragment that has the most influence on the ESIPT of HPBI in the $^1n\pi^*$ state. Thus, it is concluded that salicylamine is the smallest model system for a qualitative study of the intramolecular proton

transfer of HPBI in the ground, $^1\pi\pi^*$, and $^3\pi\pi^*$ excited states and HPI or HVBI is needed if one also wants a qualitative ESIPT description of HBPI in the $^1n\pi^*$ state.

Finally, rotamerism in HPI in the ground and $^1\pi\pi^*$ excited states is similar to that found in HPBI. The enol cis and trans rotamers are interconvertible in the ground state but not in the first excited state. In HVBI the interconversion is more inhibited both in the ground and the first excited state.

Acknowledgment. This work has been funded in part through the Spanish DGICYT Project No. PB95-0762 and the European Union Project No. CII*-CT93-0339. One of us (M.F.) thanks the Generalitat de Catalunya for financial help through CIRIT Project No. FI/96-05011.1.

Supporting Information Available: Table listing coordinates and total energies for all optimized minima and transition states in the ground and $^1\pi\pi^*$, $^1n\pi^*$, and $^3\pi\pi^*$ excited states of HPVI and HPI. This material is available free of charge via the Internet at <http://pubs.acs.org>.

References and Notes

- Williams, D. L.; Heller, A. *J. Phys. Chem.* **1970**, *74*, 4473.
- Woolfe, G. J.; Melzig, M.; Schneider, S.; Door, F. *Chem. Phys.* **1983**, *77*, 213.
- Arthen-Engeland, Th.; Bultman, T.; Ernsting, N. P.; Rodriguez, M. A.; Thiel, W. *Chem. Phys.* **1992**, *163*, 43.
- Lavtchieva, L.; Enchev, V.; Smedarchina, Z. *J. Phys. Chem.* **1993**, *97*, 306.
- Nagaoka, S.; Ithoh, A.; Mukai, K.; Nagashima, U. *J. Phys. Chem.* **1993**, *97*, 11385.
- Enchev, V. *Indian J. Chem.* **1994**, *33B*, 336.
- Barbara, P. F.; Brus, L. E.; Rentzepis, P. M. *J. Am. Chem. Soc.* **1980**, *102*, 5631.
- Ding, K.; Courtney, S. J.; Strandjord, A. J.; Friedrich, D.; Barbara, P. F. *J. Phys. Chem.* **1983**, *87*, 1184.
- Laermer, F.; Elsaesser, T.; Kaiser, W. *Chem. Phys. Lett.* **1988**, *148*, 119.
- Chou, P.; Martínez, M. L.; Studer, Sh. L. *Chem. Phys. Lett.* **1992**, *195*, 586.
- Catalán, J.; Fabero, F.; Guijarro, M. S.; Claramunt, R. M.; Santa-María, M. D.; Foces-Foces, M. C.; Hernández-Cano, F.; Elguero, J.; Sastre, R. *J. Am. Chem. Soc.* **1990**, *112*, 747.
- Das, K.; Sarkar, N.; Majumdar, D.; Bhattacharyya, K. *Chem. Phys. Lett.* **1992**, *198*, 443.
- Das, K.; Sarkar, N.; Ghosh, A. K.; Majumdar, D.; Nath, D. N.; Bhattacharyya, K. *J. Phys. Chem.* **1994**, *98*, 9126.
- Sinha, H. K.; Dogra, S. K. *Chem. Phys.* **1986**, *102*, 337.
- Rodríguez, F.; Ríos, M. C.; Mosquera, M.; Ríos, M. A. *J. Phys. Chem.* **1994**, *98*, 8666.
- Barbara, P. F.; Walsh P. K.; Brus, L. E. *J. Phys. Chem.* **1989**, *93*, 29.
- Wiechmann, M.; Port, H.; Frey, W.; Larmer, F.; Elsasser, T. *J. Phys. Chem.* **1991**, *95*, 1918.
- Wiechmann, M.; Port, H.; Larmer, F.; Frey, W.; Elsasser, T. *Chem. Phys. Lett.* **1990**, *165*, 28.
- Itoh, M.; Fuziwara, Y. *J. Am. Chem. Soc.* **1985**, *107*, 1561.
- McMorrow, D.; Kasha, M. *J. Phys. Chem.* **1984**, *88*, 2235.
- Sengupta, P. K.; Kasha, M. *Chem. Phys. Lett.* **1979**, *68*, 382.
- Brinn, I. M.; Carvallo, C. E. M.; Heisel, F.; Mieche, J. A. *J. Phys. Chem.* **1991**, *95*, 6540.
- Chou, P. T.; Martínez, M. L. *J. Phys. Chem.* **1992**, *96*, 2018.
- Acuña, A. U.; Amat, F.; Catalán, J.; Costela, A.; Figuera, J. M.; Muñoz, J. M. *Chem. Phys. Lett.* **1986**, *132*, 567.
- Swinney, T. C.; Kelley, D. F. *J. Phys. Chem.* **1991**, *95*, 10369.

- (26) Brucker, G. A.; Swinney, T. C.; Kelly, D. F. *J. Phys. Chem.* **1991**, 95, 3190.
- (27) Al-Soufi, W.; Grellmann, K. H.; Nickel, B. *J. Phys. Chem.* **1991**, 95, 10503.
- (28) Eisenberger, H.; Nickel, B.; Andreas Ruth A.; Al-Soufi, W.; Grellmann, K. H.; Novo, M. *J. Phys. Chem.* **1991**, 95, 10509.
- (29) Strandjord, A. J. G.; Barbara, P. F. *J. Phys. Chem.* **1985**, 89, 2335.
- (30) Cho, D.; Tian, R.; Porter, L. J.; Hemingway, R. W.; Mattice, W. L. *J. Am. Chem. Soc.* **1990**, 112, 4273.
- (31) Felker, P. M.; Lambert, W. R.; Zewail, A. H. *J. Chem. Phys.* **1982**, 77, 1603.
- (32) Herek, J. L.; Pedersen, S.; Bañares, L.; Zewail, A. H. *J. Chem. Phys.* **1992**, 97, 9046.
- (33) Douhal, A.; Lahmani, F.; Zehnacker-Rentien, A. *Chem. Phys.* **1993**, 178, 493.
- (34) Makri, N.; Miller, W. H. *J. Chem. Phys.* **1989**, 91, 4026.
- (35) Bosch, E.; Moreno, M.; Lluch, J. M. *Chem. Phys.* **1992**, 159, 99.
- (36) Douhal, A.; Lahmani, F.; Zewail, A. H. *Chem. Phys.* **1996**, 207, 477.
- (37) Heller, H. J.; Blattmann, H. R. *Pure Appl. Chem.* **1973**, 36, 141.
- (38) Durr, H.; Bouas-Laurent, H., Eds.; *Photochromism. Molecules and Systems*; Elsevier: Amsterdam, 1990; Chapters 16 and 17.
- (39) Werner, T. *J. Phys. Chem.* **1979**, 83, 320.
- (40) Khan, A. U.; Kasha, M. *Proc. Natl. Acad. Sci. U.S.A.* **1983**, 80, 1767.
- (41) Chou, P. T.; McMorro, D.; Aartsma, T. J.; Kasha, M. *J. Phys. Chem.* **1984**, 88, 4596.
- (42) Parthenopoulos, D. A.; McMorro, D.; Kasha, M. *J. Phys. Chem.* **1991**, 95, 2668.
- (43) Acuña, A. U.; Costela, A.; Muñoz, J. M. *J. Phys. Chem.* **1986**, 90, 2807.
- (44) Acuña, A. U.; Amat, F.; Catalán, J.; Costela, A.; Figuera, J. M.; Muñoz, J. M. *Chem. Phys. Lett.* **1986**, 132, 567.
- (45) Costela, A.; Amat, F.; Catalán, J.; Douhal, A.; Figuera, J. M.; Muñoz, J. M.; Acuña, A. U. *Opt. Commun.* **1987**, 64, 457.
- (46) Costela, A.; Muñoz, J. M.; Douhal, A.; Figuera, J. M.; Acuña, A. U. *Appl. Phys. B* **1989**, 49, 545.
- (47) Das, K.; Sarkar, N.; Majumdar, D.; Bhattacharyya, K. *Chem. Phys. Lett.* **1993**, 204, 393.
- (48) Sobolewski, A. L.; Domcke, W. *Chem. Phys. Lett.* **1993**, 211, 82.
- (49) Forés, M.; Duran, M.; Solà, M. *Chem. Phys.* **1998**, 234, 1.
- (50) Ríos, M. A.; Ríos, M. C. *J. Phys. Chem. A* **1998**, 102, 1560.
- (51) Forés, M.; Duran, M.; Solà, M.; Orozco, M.; Luque, F. J. *J. Phys. Chem.* in press.
- (52) Foresman, J. B.; Head-Gordon, M.; Pople, J. A.; Frisch, M. J. *J. Phys. Chem.* **1992**, 96, 135.
- (53) Luth, K.; Scheiner, S. *J. Phys. Chem.* **1994**, 98, 3582.
- (54) Luth, K.; Scheiner, S. *J. Phys. Chem.* **1995**, 99, 7352.
- (55) Scheiner, S.; Kar, T.; Cuma, M. *J. Phys. Chem. A* **1997**, 101, 5901.
- (56) Rovira, M. C.; Scheiner, S. *J. Phys. Chem.* **1995**, 99, 9854.
- (57) Forés, M.; Duran, M.; Solà, M.; Adamowicz, L., submitted for publication.
- (58) Barone, V.; Adamo, C. *Int. J. Quantum. Chem.* **1997**, 61, 429.
- (59) Frisch, M. J.; Trucks, G. W.; Schlegel, H. B.; Gill, P. M. W.; Johnson, B. G.; Robb, M. A.; Cheeseman, J. R.; Keith, T. A.; Petersson, G. A.; Montgomery, J. A.; Raghavachari, K.; Al-Laham, M. A.; Zakrewski, V. G.; Ortiz, J. V.; Foresman, J. B.; Cioslowski, J.; Stefanov, B.; Nanayakkara, A.; Challacombe, M.; Peng, C. Y.; Ayala, P. Y.; Chen, W.; Wong, M. W.; Andrés, J. L.; Replogle, E. S.; Gomperts, R.; Martin, R. L.; Fox, D. J.; Binkley, J. S.; Defrees, D. J.; Baker, J.; Stewart, J. J. P.; Head-Gordon, M.; Gonzalez, C.; Pople, J. A. GAUSSIAN 94, Revision B.2; Gaussian Inc.: Pittsburgh, PA, 1995.
- (60) Dunning, T. H., Jr.; Hay, P. J. In *Methods of electronic structure theory*; Schaefer, H. F., Ed.; Plenum Press: New York, 1977.
- (61) Cuma, M.; Scheiner, S.; Kar, T. *J. Mol. Struct. (THEOCHEM)*, in press.
- (62) Forés, M.; Scheiner, S. *Chem. Phys.*, in press.
- (63) Guallar, V.; Moreno, M.; Lluch, J. M.; Amat-Guerri, F.; Douhal, A. *J. Phys. Chem.* **1996**, 100, 19789.
- (64) Douhal, A.; Amat-Guerri, F.; Lillo, M. P.; Acuña, A. U. *J. Photochem. Photobiol. A: Chem.* **1994**, 78, 127.
- (65) Foces-Foces, C.; Llamas-Saiz, A. L.; Claramunt, R. M.; Cabildo, P.; Elguero, J. *J. Mol. Struct. (THEOCHEM)* **1998**, 440, 193.